M. Knud HENRICHSEN E-6

LEP note 168
28.6.79

Current dependent phenomena in LEP

A. Hofmann and J.R. Maidment *

1) Introduction

The interaction of the beam with its surroundings leads to current dependent phenomena such as parasitic mode losses, bunch lengthening, frequency shifts and instabilities. Since LEP has a very large radius and only few bunches the peak current of the beam is large and the related single bunch effects very pronounced. Coupled bunch effects, however, are rather weak because of the large bunch spacing. Radiation damping suppresses most of those instabilities. The growth rate of most instabilities is calculated without taking damping into account. The results are then compared with the existing Landau and radiation damping.

2) Impedance estimates

The part played by the wall in its interaction with the beam can be described by a frequency dependent impedance. The longitudinal impedance $Z_L(\omega)$ is the voltage per turn induced by a unit current at a frequency ω. The transverse impedance [1, 2] $Z_T(\omega)$ is defined as the transversely acting fields, integrated over one revolution, which are induced by a unit current with unit displacement

$$Z_T(\omega) = j \, \frac{\int_0^{2\pi R} [\vec{E} + \vec{v} \times \vec{B}]_T \, ds}{\beta I \Delta x}$$

with $v = \beta c$ = velocity of the particle, Δx = transverse displacement, I = beam current; R = average radius. These impedances have a resistive (real) part $Z_R(\omega)$, responsible for parasitic energy losses and growth rates of instabilities, and a reactive (imaginary) part $Z_I(\omega)$ which causes frequency shifts and potential well distortions. The parasitic energy loss depends on the longitudinal impedance itself which increases with the size of the

* Rutherford Laboratory

machine. Longitudinal instabilities and bunch lengthening are given by the impedance divided by the mode number $\frac{Z_L(\omega)}{r}$, ($r = \omega/\omega_o$; ω_o = revolution frequency) which depends only on the impedance per unit length and does not increase with the machine size. The transverse impedance $Z_T(\omega)$, however, scales again with the radius of the machine.

LEP version 8 has a circumference of 30608 m with 28700 m of vacuum chambers and 768 cavities. The cross section of the vacuum chamber can be approximated by an ellipse with the full axises W = 0.138 m and H = 0.076 m. The chamber consists of aluminium with a resistivity

$$\rho_R \approx 0.029 \cdot 10^{-6}\ \Omega m .$$

The narrow band impedances, which drive coupled bunch mode instabilities, are due to single parasitic resonances in the RF-cavities or other objects. The estimation of these impedances is based on computations.

The broad band impedance, which causes single bunch effects, is due to aperture changes, bellows etc. and due to the sum effect of many parasitic resonances in the cavities. This broad band impedance usually increases first with frequency[3] until the cut off frequency of the lowest mode is approached and wave propagation in the chamber becomes possible. (For the LEP vacuum chamber this cut off frequency is about 1.3 GHz for the lowest transverse mode and about 2.6 GHz for the lowest longitudinal mode). Above this frequency the impedance decreases again. For the RF-cavities the longitudinal broad band impedance has been estimated by summing over the computed parasitic resonances. For the vacuum chamber it has been assumed that the impedance per unit length is the same as for the very similar PETRA chamber. The transverse broad band impedance has been obtained from the longitudinal one using an approximate general relation between the two.

Finally the smooth wall impedance due to skin effect has been calculated for the given properties of the vacuum chamber.

The cavity impedance at the RF-frequency itself (basic mode) is not considered here since its effects are an integer part of the RF beam dynamic (beam loading). However due to the finite band width, this impedance extends beyond the first few revolution side bands and can make some longitudinal coupled bunch modes unstable. The impedance of the higher harmonic cavities is also ignored since it is small compared to the one of the main RF-cavities.

2.2 Narrow band impedances

The longitudinal impedance of a single resonator with resonant frequency ω_r, quality factor Q_r and shunt impedance R_s has the form

$$Z_L(\omega) = \frac{R_{LS}}{1 - j\,Q_r\left(\frac{\omega_r}{\omega} - \frac{\omega}{\omega_r}\right)} \tag{2.1}$$

and

$$\frac{Z_L(\omega)}{r} = \frac{R_{LS}\,\omega_0}{\omega_r}\;\frac{\left(\omega/\omega_r + j\,Q_r\left(1-(\omega/\omega_r)^2\right)\right)}{(\omega/\omega_r)^2 + Q_r^2\left(1-(\omega/\omega_r)^2\right)^2}\,. \tag{2.2}$$

The transverse impedance of a deflecting mode resonance has the same form as (2.2)

$$Z_T(\omega) = R_{TS}\;\frac{\omega/\omega_r + j\,Q_r\left(1-(\omega/\omega_r)^2\right)}{(\omega/\omega_r)^2 + Q_r^2\left(1-(\omega/\omega_r)^2\right)^2} \tag{2.3}$$

The parasitic modes in an RF-cavities cell have been computed[5,6] using the programs KN7C[7] and SUPERFISH[8] up to a frequency of $\approx$ 2.5 GHz. Their properties are listed in ref. 6 and indicated on fig. 1a).

For the lowest and strongest mode in one cell we have the parameters
$\omega_{r1}/2\pi = 525$ MHz, $Q_{r1} = 40500$, $R_{LS1}/Q_{r1} = 55.6$

To find the total effect of all 3840 cells in the whole LEP RF system we have to take into account that there is a spread in the resonance frequencies of the cells due to the finite tollerances in the cavity construction. This will result in an "effective" quality factor Q_r of the whole RF system which is lower than the one of a single cell. The total R_{LS}/Q_r however will be the sum of the single contributions. Assuming a tollerance of 0.1 mm we estimate the effective Q_r to be about 3000 resulting in a total shunt impedance $R_{LS} \simeq 640$ MΩ.

To obtain the transverse narrow band impedance the lowest deflecting mode in an RF-cell has been calculated[7] with the result $\omega_{r1}/2\pi = 565$ MHz and $R_{TS1} = 15.2$ MΩ/m. The quality factor has been estimated to be about 40000. Using the same criteria as for the longitudinal case we find for the total effect of this mode

$Q_r = 3000$ and $R_{TS} = 4.4$ GΩ/m.

The longitudinal impedance of the RF-cavities at the RF-frequency itself is ignored in the present consideration since it is an integer part of beam loading treated in the RF-beam dynamics. However this mode has a finite width which represents a sizable impedance over several revolution frequency bands. This can drive coupled bunch mode instabilities. The LEP RF-system consists of the accelerating cavities and the storage cavities. This coupled system has 2 resonant frequencies at around 4 revolution frequencies below and above the actual RF-frequency. There is slight detuning such that these 2 frequencies are 1.1 KHz below the next harmonic of the revolution frequency.

The parameters of this impedance are shown in table 1b).

2.3 Broad band impedance

The longitudinal broad band impedance of the RF-system is estimated by averaging the resistive part of the computed parasitic resonances over a certain frequency bin $\Delta\omega$.

$$Z_{LR}(\omega)_{\text{broad band}} = \frac{1}{2\Delta\omega}\int_{\omega-\Delta\omega/2}^{\omega+\Delta\omega/2} Z_R(\omega)_p \, d\omega = \frac{1}{2}\sum \frac{\pi}{2}\,\omega_{rp}\left(\frac{R_s}{Q_r}\right)_p \tag{2.4}$$

where $Z_R(\omega)_p$ is the resistive impedance of the computed modes and $\frac{\pi}{2}\omega_{rp}\left(\frac{R_s}{Q_r}\right)_p$ the area of a single resonance p. The factor $\frac{1}{2}$ in front takes into account that for a single passage through an empty cavity, the bunch has to build the fields up first and sees in average only half of the computed field. The contributions (2.4) of the single modes and their average over 250 MHz bins is shown in fig. 1. This impedance is fitted with the one of a resonator with $Q_r = 1$, $\omega_r/2\pi = 1.3$ GHz and $R_{LS} = 0.468$ MΩ. This resonator fit approximates the impedance quite well but is mostly done for convenience since many computations can be carried out easily for this type of impedance. The resistive (real) and reactive (imaginary) as well as the absolute value of such an impedance divided by mode number are shown on fig. 2 and are given by

$$\frac{Z_L(\omega)}{r}_{\text{broad band}} = \left|\frac{Z}{r}\right|_0 \frac{\omega_r^2\left(\omega\,\omega_r + j\,(\omega_r^2-\omega^2)\right)}{\omega^4 - \omega^2\omega_r^2 + \omega_r^4} \tag{2.5}$$

where $\left|\frac{Z}{r}\right|_0 = R_s \cdot \frac{\omega_0}{\omega_r}$

is the absolute value of the impedance at low frequency. This is independent of the machine radius and is a suitable quantity to describe the broad band impedance of a storage ring. For the contribution of the vacuum chamber to the broad band impedance we use also a resonator fit with the same ω_r and Q_r and with a shunt impedance $R_{LS} = 0.149$ MΩ. This gives the same parasitic mode loss parameter per unit length as measured for the very similar PETRA vacuum chamber [4]; see next section.

The transverse broad band impedance has been estimated from the longitudinal one using the approximate relation between the two [1,9]

$$Z_T(\omega) = \frac{2R}{b^2}\,\frac{Z_L}{r}(\omega)$$

where b is the effective radius of the chamber. For an elliptical cross section we obtain for the "vertical" effective radius

$$b_{vac} = \frac{H/2}{\left(2\,(\xi_1 - \varepsilon_1)\right)^{1/3}} = 0.04\ \text{m} \tag{2.6}$$

where ξ_1 and ε_1 are the Laslett coefficients[10]. This gives a vertical broad band impedance for the vacuum chamber of $R_{TS(vac)} = 6.86$MΩ/m.

For the RF-cavities we use for b the full inside radius of the cell b = 0.3m and get $R_{TS(cav.)} = 0.38$MΩ/m. This choice of effective radius is not well founded and could be optimistic. However the choice is not very critical since even for b = 0.15m the contribution of the cavities to the transverse impedance would be small compared to the one of the vacuum chamber.

All broad band impedances are listed in table 1.c).

2.4 The smooth resistive wall impedance

At very low frequencies the impedance given by the skin effect in the smooth wall becomes important.

It is given by

$$\frac{Z_L}{r}(\omega)_{skin} = \frac{c}{b}\sqrt{\frac{\varrho_R \mu_o}{2|\omega|}}\left(1 \cdot \mathrm{sign}(\omega) + j\right)$$

and

$$Z_T(\omega)_{skin} = \frac{2cR}{b^3}\sqrt{\frac{\varrho_R \mu_o}{2|\omega|}}\left(1 \cdot \mathrm{sign}(\omega) + j\right) .$$

The values of the resistive part of these impedances are given in table 1d).

They scale like $\omega^{-1/2}$

Table 1. Summary of the estimated impedances

a) Lowest narrow band parasitic resonances

	$\omega_r/2$, (MHz)	Q_r	strength
longitudinal	525	3000	R_{SL} = 640 MΩ
transverse	565	3000	R_{TS} = 4.46 GΩ/m

b) Basic mode of the RF-system, (coupled accelerating and storage cavities)

ω_r/ω_o	Q_r	R_s (GΩ)
36075.89	40 000	32.5
36083.89	40 000	32.5

c) Broad band impedance, (resonator fit with $\omega_r/2\pi \simeq 1.3$ GHz, $Q_r = 1$)

	longitudinal		transverse
	R_{LS}, (MΩ)	$\|Z/r\|_o$, (Ω)	R_{TS} (MΩ/m)
vacuum chamber	0.145	1.12	6.86
cavities	0.468	3.53	0.38
total	0.617	4.65	7.24

a) Smooth resistive wall impedance at the rev. frequ.

longitudinal $\frac{Z_{LR}}{r}(\omega_o)_{skin}$ Ω	transverse $Z_{TR}(\omega_o)_{skin}$ MΩ/m
4.1	25

3. Parasitic mode losses

The longitudinal, restive broad band impedance leads to an energy loss U_{pm} per turn.

$$U_{pm} = e\, I_o\, Z_{pm}(\sigma) = \frac{e\, I_o\, 2\pi}{k_b\, \omega_o}\, k_{pm}(\sigma)$$

where I_o = total average current of all k_b bunches; $Z_{pm}(\sigma)$ = parasitic mode loss impedance, $k_{pm}(\sigma)$ = parasitic mode loss parameter. Both Z_{pm} and k_{pm} depend on the bunch length σ. For a Gaussian bunch this loss parameter is [11)]

$$k_{pm}(\sigma) = \frac{1}{\pi} \int_0^\infty Z_{LR}(\omega)\, \exp(-\omega^2\sigma^2/c^2)\, d\omega$$

For our resonator fit of the broad band impedance we get

$$k_{pm}(x_r) = \frac{R_s\, c}{\pi\, \sigma} \int_0^\infty \frac{x_r^2\, x^2\, e^{-x^2}}{x^4 - x^2 x_r^2 + x_r^4}\, dx \tag{3.1}$$

with

$$x = \frac{\omega\, \sigma}{c} \quad , \quad x_r = \frac{\omega_r\, \sigma}{c}\, . \tag{3.2}$$

The integral in (3.1) is listed in table 2.

This loss parameter caused by the vacuum chamber has been measured in PETRA[4)] for a bunch length $\sigma = 3.7$cm and found to be $k_{pm} = 10.5$ GΩ s^{-1}.

Scaling this with the size of the machine we get from (3.1) for the very similar LEP vacuum chamber $R_{LS\ vac} = 0.149$ MΩ which has been used in section 2.3. For a bunch length of $\sigma = 2.5$cm we obtain for LEP Z_{pm} (2.5cm) = 24 GΩ. The dependence on σ can be approximated by

$Z_{pm} \propto \sigma^{-1.23}$.

4) Potential well and turbulent bunch lengthening for the standard RF-system

4.1) Bunch form

For a single RF-system we approximate the RF wave form by

$$V(\Phi) = V_o \left(\cos\Phi \cdot \Phi + \sin \Phi_s\right) \tag{4.1}$$

where Φ is the phase angle measured from the bunch center, and Φ_s the synchronous phase angle ($\cos\Phi_s \leq 0$ above transition energy).

The instantaneous current $I(s)$ as a function of the longitudinal coordinate $s = \frac{-R}{h}\Phi$ is

$$I(s) = I_p \exp\left(-\frac{s^2}{2\sigma^2}\right) = \frac{\sqrt{2\pi}\, R I_o}{k_b\, \sigma} \exp\left(-\frac{s^2}{2\sigma^2}\right) \tag{4.2}$$

with I_p = peak current.

4.2) Potential well (inductive wall effect)

We consider a reactive impedance which is predominantly inductive and calculate its effect on the bunch length and incoherent phase oscillation frequency[12]. The field induced in the inductive impedance with inductance $\frac{dL}{ds'}$ per unit length is

$$E_s = \frac{dL}{ds'}\, c \cdot \frac{dI}{ds} \approx \frac{dL}{ds'}\, c\, \frac{I_p}{\sigma^2}\, s \tag{4.3}$$

where we developed (4.2) and took only the first term since the effect acts mainly on the core of the bunch. The induced voltage V_{in} per revolution seen by a particle inside the bunch one is obtained by integrating (4.3) over the circumference

$$V_{in} = -L\, I_p\, c\, \frac{s}{\sigma^2} = -\frac{I_p R \omega_o L s}{\sigma^2} = -\frac{\sqrt{2\pi}\, R^2 I_o}{k_b\, \sigma^3} \frac{Z_I}{r}\, s \tag{4.4}$$

where $\frac{Z_I}{r} = L\omega_o$ is the inductive impedance divided by the mode number and L the total inductance of the ring. The induced voltage (4.4) has to be added to the external RF-voltage (4.1)

$$V(\phi) = V_o \cos\phi_s \left[1 + \frac{\sqrt{2\pi}\, I_o\, Z_I/r}{k_b\, h\, V_o \cos\phi_s} \left(\frac{R}{\sigma}\right)^3\right]\phi + V_o \sin\phi_s$$

The inductive wall leads to a reduction of the RF voltage seen by a particle inside the bunch and hence to a decrease of the incoherent phase oscillation frequency ω_s and to an increase of the bunch length compared to the natural values ω_{so} and σ_o .

From

$$\omega_s^2 \propto \left|\frac{dV}{d\phi}\right| \qquad \text{we get}$$

$$\left(\frac{\omega_s}{\omega_{so}}\right)^2 = \left(\frac{\sigma_o}{\sigma}\right)^2 = 1 + \frac{\sqrt{2\pi}\, I_o\, Z_I/r}{k_b\, h\, V_o \cos\phi_s}\left(\frac{R}{\sigma}\right)^3 = 1 - \frac{e}{\sqrt{2\pi}\, k_b}\, \frac{\alpha\, I_o\, Z_I/r}{Q_{so}^2\, E}\left(\frac{R}{\sigma}\right)^3 \tag{4.6}$$

with α = momentum compaction factor, E = particle energy and

$$Q_{so}^2 = \left(\frac{\omega_{so}}{\omega_o}\right)^2 = \frac{h\,\alpha\, e\, V_o\, |\cos\phi_s|}{2\pi\, E}$$

From (4.6) we get an equation which describes the potential well bunch lengthening

$$\left(\frac{\sigma}{\sigma_o}\right)^3 - \left(\frac{\sigma}{\sigma_o}\right) - \frac{e}{\sqrt{2\pi}\, k_b}\, \frac{\alpha\, I_o\, Z_I/r}{Q_{so}^2\, E}\left(\frac{R}{\sigma_o}\right)^3 = 0 \tag{4.7}$$

We assumed here a reactive impedance which is mainly inductive and approximated the Gaussian distribution by a parabolic one. In this case the potential well increases the length of the bunch without changing its shape [12, 13]. For a general reactive impedance the situation is more complicated. To keep things simple we will use an effective impedance

$$\left(\frac{Z_I}{r}\right)_{eff} = \int_0^{\infty} \frac{Z_I}{r}(\omega)\; h(\omega)\, d\omega$$

where Z_I is the reactive impedance and $h(\omega)$ the power spectrum of the Gaussian bunch

$$h(\omega) = \frac{\sigma}{\sqrt{\pi}\, c}\, \exp\left(-\omega^2\sigma^2/c^2\right) \quad ; \quad \int_{-\infty}^{\infty} h(\omega)\, d\omega = 1 \tag{4.8}$$

For our broad band resonator impedance (2.5) we get

$$\left(\frac{Z_I}{r}\right)_{eff} = \left|\frac{Z}{r}\right|_o \frac{2x_r^2}{\sqrt{\pi}} \int_0^{\infty} \frac{(x_r^2 - x^2)\, e^{-x^2}}{x^4 - x^2 x_r^2 + x_r^4}\, dx \tag{4.9}$$

The potential well bunch lengthening is calculated by replacing $\frac{Z_I}{r}$ in (4.7) by $\left(\frac{Z_I}{r}\right)_{eff}$ given by (4.9).

4.3) Turbulent bunch lengthening

For turbulent bunch lengthening in the absence of potential well we use the coasting [14] beam model and apply the Keil-Schell criterion[15] to the local energy spread and current

$$\left|\frac{Z}{r}\right| = F' \frac{E\alpha}{e} \frac{(\sigma_E/E)^2}{I_p} \tag{4.10}$$

Above the turbulent threshold we get for the equilibrium bunch length

$$\left(\frac{\sigma}{R}\right)^3 = \frac{\sqrt{2\pi}}{F'} \frac{e}{k_b} \frac{\alpha I_0}{Q_s^2 E} \left|\frac{Z}{r}\right| \tag{4.11}$$

and the energy spread

$$\left(\frac{\sigma_E}{E}\right)^3 = \left(\frac{Q_s \sigma}{\alpha R}\right)^3 = \frac{\sqrt{2\pi}}{F'} \frac{e}{k_b} \frac{Q_s I_0}{\alpha^2 E} \left|\frac{Z}{r}\right| \tag{4.12}$$

The form factor F' has a value of $\sim 2\pi$ for a Gaussian bunch. The threshold current I_{th} is

$$I_{th} = \frac{F' k_b}{\sqrt{2\pi} e} \frac{Q_{so}^2 E}{\alpha |Z/r|} \left(\frac{\sigma_c}{R}\right)^3 \tag{4.13}$$

The impedance $\left|\frac{Z}{r}\right|$ depends on the frequency ω. It is not clear at what frequency $\left|\frac{Z}{r}\right|$ should be evaluated. Low frequencies with wave length much longer than the bunch are not effective to create turbulence. We make here an arbitrary choice to evaluate $|Z/r|$ at the frequency

$$\omega_{crit.} = \frac{c}{\sigma} \quad ; \quad \left|\frac{Z}{r}\right|_{crit.} = \left|\frac{Z}{r}(\omega_{crit.})\right| \tag{4.14}$$

which is one standard deviation of the bunch spectrum (4.8). This choice is not very critical for long bunches where $|Z/r|$ depends little on σ as shown in fig. 2. A more detailed discussion of this problem can be found in ref. 16).

For our broad band resonator impedance we get for $|Z/r|_{crit.}$

$$\left|\frac{Z}{r}\right|_{crit} = \left|\frac{Z}{r}\right|_0 \frac{x_r^2}{\sqrt{x_r^4 - x_r^2 - 1}}$$

The ratio $|Z/r|_{crit.}/|Z/r|_0$ is listed in table 2.

4.4 Combined potential well and turbulent bunch lengthening

To account for the effect of the inductive wall in the presence of turbulence we express Q_s in (4.11) by its natural value Q_{so} using (4.6) and get for the total bunch length

$$\left(\frac{\sigma_t}{R}\right)^3 = \frac{e}{\sqrt{2\pi}\, k_b} \frac{\alpha I_o}{Q_{so}^2 E} \left|\frac{Z}{r}\right|_o \frac{|Z/r|_{crit} + (Z_I/r)_{eff.}}{|Z/r|_o} \tag{4.15}$$

At the turbulent threshold the total bunch length given by (4.15) must be equal to the potential well bunch length (4.7). This gives for the threshold bunch length σ_{th}

$$\frac{\sigma_{th}}{\sigma_o} = \left(1 + \frac{(Z_I/r)_{eff}}{|Z/r|_{crit.}}\right)^{1/2} \tag{4.16}$$

and for the threshold current

$$I_{th} = \frac{\sqrt{2\pi}\, k_b}{e} \frac{Q_{so}^2 E}{\alpha\, |Z/r|_{crit.}} \left(\frac{\sigma_o}{R}\right)^3 \sqrt{1 + \frac{(Z_I/r)_{eff}}{|Z/r|_{crit}}} \tag{4.17}$$

The phase oscillation frequency above the turbulent threshold is

$$\frac{\omega_s}{\omega_{so}} = \left(1 + \frac{(Z_I/r)_{eff.}}{|Z/r|_{crit.}}\right)^{-1/2} \tag{4.18}$$

and the increase in momentum spread

$$\left(\frac{\sigma_E}{\sigma_{E_o}}\right)^3 = \frac{e}{\sqrt{2\pi}\, k_b} \frac{Q_{so} I_o}{\alpha^2 E} \left|\frac{Z}{r}\right|_{crit.} \left(1 + \frac{(Z_I/r)_{eff}}{|Z/r|_{crit}}\right)^{-1/2} \tag{4.19}$$

or

$$\frac{\sigma_E}{\sigma_{E_o}} = \left(1 + \frac{(Z_I/r)_{eff.}}{|Z/r|_{crit}}\right)^{-1/2} \left(\frac{\sigma}{\sigma_o}\right)$$

Due to the dependence of the impedance on bunch length these equations have to be solved by iteration.

4.5 Approximation for long bunches

If the bunch length is large

$$\sigma > \frac{c}{\omega_r} \qquad (\approx 3.7\,\mathrm{cm} \text{ for LEP})$$

we can approximate

$$\left(\frac{Z_I}{r}\right)_{eff} \approx \left|\frac{Z}{r}\right|_{crit} \approx \left|\frac{Z}{r}\right|_{o}$$

and simplify the equations. We get for the threshold bunch length

$$\frac{\sigma_{th}}{\sigma_o} \approx \sqrt{2}$$

and for the phase oscillation frequency in the presence of turbulence

$$\frac{\omega_s}{\omega_{so}} \approx \frac{1}{\sqrt{2}} .$$

For shorter bunches the critical and effective impedance are smaller than the absolute value. The effect of the potential well should then be smaller.

5. Bunch lengthening for the double RF-system

5.1 Bunch form

We assume a double RF-system with the frequencies ω_{RF} and $N\omega_{RF}$ operating in the bunch lengthening mode[17]. The RF wave form can be approximated by

$$V(\phi) = V_o \left(\frac{N^2-1}{6}\right) \cos\Phi_s \cdot \phi^3 + V_o \left(1-\frac{1}{N^2}\right) \sin\Phi_s \tag{5.1}$$

where V_o and Φ_s are the voltage and the synchronous phase angle of the main RF-system. The instananeous current $I(s)$ is

$$I(s) = I_p \exp\left(-A_1 \frac{s^4}{\sigma^4}\right) = C_1 \frac{R I_o}{k_b \sigma} \exp\left(-A_1 \frac{s^4}{\sigma^4}\right) \tag{5.2}$$

with $$A_1 = \frac{2\pi^2}{(\Gamma(1/4))^4} = 0.11426 \quad ; \quad \Gamma(1/4) = 3.6254,$$

and

$$C_1 = \frac{4\pi\sqrt{2\pi}}{\sqrt[4]{2}\,(\Gamma(1/4))^2} = 2.015 .$$

Here σ is the rms-bunch length. The power spectrum $h(\omega)$ of this bunch (5.2) had to be calculated numerically and is shown in fig. 3 together with the squared spectrum of a Gaussian bunch with the same σ. For the bunch (5.2) the rms frequency of its power spectrum is

$$\text{rms}\ (\omega) \quad = \quad 0.98\ \frac{c}{\sigma}$$

while the corresponding number for a Gaussian bunch is

$$\text{rms}\,(\omega)_{\text{Gauss}} \quad = \quad \frac{c}{\sigma}$$

Due to the similarity of the two power spectra $h(\omega)$ we use the same effective and critical impedances as in the last chapter.

5.2) Potential well (inductive wall effect).

With a predominantly inductive reactive impedance we get for the induce voltage per turn

$$V_{in} = -\frac{4A_1 I_p R}{\sigma^4}\left(\frac{Z_I}{r}\right)_{\text{eff}} \cdot s^3 = \frac{4A_1 C_1 I_o}{k_b h^3}\left(\frac{R}{\sigma}\right)^5\left(\frac{Z_I}{r}\right)_{\text{eff}} \cdot \Phi^3 \tag{5.4}$$

The total voltage is

$$V(\phi) = V_o\left(\frac{N^2-1}{6}\right)\cos\phi_s\left[1 - \frac{A_2\ I_o\ e\alpha (Z_I/r)_{\text{eff}}}{k_b\ h^2 (N^2-1)\ Q_{so}^2\ E}\left(\frac{R}{\sigma}\right)^5\right]\phi^3$$

$$+\ V_o\left(1-\frac{1}{N^2}\right)\sin\Phi_s \tag{5.5}$$

with

$$A_2 = \frac{24A_1C_1}{2\sigma} = 0.8794\ ;\ Q_{so}^{\ 2} = \frac{h\alpha eV_o\,|\cos\phi_s|}{2\pi E}\ .$$

The inductive impedance reduces the effective RF-voltage, decreases the phase oscillation frequency and increases the bunch length. The situation is somewhat more complicated than in the case of a single RF-system because the frequency depends on the amplitude of the energy oscillation ΔE For a given amplitude the frequency will be reduced by the factor

$$\left(\frac{\omega_s}{\omega_{so}}\right)^4 = 1 - \frac{A_2\ e\ \alpha\ I_o\ (Z_I/r)_{\text{eff}}}{k_b\ h^2\ (N^2-1)\ Q_{so}^2\ E}\left(\frac{R}{\sigma}\right)^5 \tag{5.6}$$

This leads to an equation describing the potential well bunch lengthening

$$\left(\frac{\sigma}{\sigma_o}\right)^5 - \left(\frac{\sigma}{\sigma_o}\right) - \frac{A_2\, e\, \alpha\, I_o\, (Z_I/r)_{eff}}{k_b\, h^2\, (N^2-1)\, E\, Q_{so}^2}\left(\frac{R}{\sigma_o}\right)^5 = 0 \qquad (5.7)$$

Where the natural bunch length is

$$\frac{\sigma_o}{R} = \frac{2\sqrt{\pi}}{\Gamma(1/4)}\sqrt[4]{\frac{3}{N^2-1}}\sqrt{\frac{\alpha\ \sigma_{Eo}/E}{h\ Q_{so}}}\ .$$

5.3 Turbulent bunch lengthening

The coasting beam model gives for the equilibrium turbulent bunch length in the absence of a potential well

$$\left(\frac{\sigma}{R}\right)^5 = \frac{2\pi A_2\ I_o\ |Z_I/r|_{crit}}{k_b\, h^3 (N^2-1)\ V_o\, |\cos\phi_s|}\ . \qquad (5.11)$$

The connected increase in energy spread is obtained from the relation

$$\frac{\sigma_E}{\sigma_{Eo}} = \left(\frac{\sigma}{\sigma_o}\right)^2 \qquad (5.12)$$

The threshold current is

$$I_{th} = \frac{k_b\, h^3\, (N^2-1)\ V_o\, |\cos\phi_s|}{2\pi A_2\ |Z/r|_{crit.}}\left(\frac{\sigma_o}{R}\right)^5\ . \qquad (5.13)$$

(5.4) Combined potential well and turbulent bunch lengthening

We replace the RF-voltage in (5,11) by the reduced voltage (5.5) and get for the total bunch length

$$\left(\frac{\sigma_t}{R}\right)^5 = \frac{A_2\, e}{k_b\, h^2 (N^2-1)} \; \frac{\alpha\, I_0\, |Z/r|_0}{Q_{s0}^{\,2}\; E} \cdot \frac{|Z/r|_{crit} + (Z_I/r)_{eff}}{|Z/r|_0} \tag{5.15}$$

Using (5.7) and (5.15) we get for the threshold length

$$\frac{\sigma_{th}}{\sigma_0} = \left(1 + \frac{(Z_I/r)_{eff}}{|Z/r|_{crit}}\right)^{1/4} \tag{5.16}$$

and current

$$I_{th} = \frac{k_b\, h^2 (N^2-1)}{A_2\, e} \; \frac{Q_{s0}^{\,2}\, E}{\alpha\, |Z/r|_{crit}} \left(\frac{\sigma_0}{R}\right)^5 \left(1 + \frac{(Z_I/r)_{eff}}{|Z/r|_{crit}}\right)^{1/4} \tag{5.17}$$

The increase in momentum spread is

$$\frac{\sigma_E}{\sigma_{E0}} = \left(1 + \frac{(Z_I/r)_{eff}}{|Z/r|_{crit.}}\right)^{-1/4} \left(\frac{\sigma}{\sigma_0}\right)^2 \tag{5.19}$$

(5.5) Approximation for long bunches

For $\sigma > \frac{c}{\omega_r}$ we can use the same approximation as in section 4.5 and get

$$\frac{\sigma_{th}}{\sigma_0} = 2^{1/4} = 1.1892$$

The influence of the potential well is small for the double RF-system and can probably be neglected in most cases.

6) Computation of bunch lengthening in LEP

The bunch length and relative increase of the energy spread has been calculated for LEP by iterating the equations (4.15) or (5.15) and (4.19) or (5.19). Up to an energy of 65 GeV the higher harmonic system has enough power to allow operation in the bunch lengthening mode and the equations in chapter 5 can be used. Above this energy the higher harmonic system can still be used to reduce the slope of RF-wave form and the phase oscillation frequency. In this case the equations of chapter 4 can be used. At the transition between the two regions some estimates had to be made.

The model used here has been compared with experimental data from existing machines. It seems that the effect of the potential well is overestimated for short bunches. The calculated turbulent bunch lengths agree about with the SPEAR data[1] but are about a factor of 1.8 larger than PETRA observations[18].

Table 2:

Parasitic mode loss integral $\frac{k_{pm}\,\pi\,\sigma}{R_{LS}\,c}$, effective reactive impedance $(Z_I/r)_{eff}$ and critical impedance $|Z/r|_{crit.}$ as a function of $x_r = \frac{\omega_r\,\sigma}{c}$.

x_r	$\frac{k_{pm}\,\pi\,\sigma}{R_{LS}\,C}$	$\frac{(Z_I/r)_{eff}}{\lvert Z/r\rvert_0}$	$\frac{\lvert Z/r\rvert_{crit.}}{\lvert Z/r\rvert_0}$
0.1	.1395	0.018	0.010
0.2	.2449	0.066	0.041
0.3	.3194	0.134	0.094
0.4	.3673	0.214	0.172
0.5	.3931	0.298	0.277
0.6	.4017	0.383	0.410
0.7	.3971	0.464	0.566
0.8	.3821	0.540	0.730
0.9	.3633	0.608	0.881
1.0	.3397	0.668	1.000
1.1	.3142	0.721	1.080
1.2	.2884	0.766	1.127
1.3	.2631	0.805	1.148
1.4	.2391	0.837	1.155
1.5	.2166	0.865	1.152
1.6	.1961	0.887	1.146
1.7	.1773	0.904	1.137
1.8	.1604	0.922	1.128
1.9	.1453	0.935	1.118
2.0	.13176	0.946	1.109

Table 3

Increase of bunch length and energy spread

E GeV	I_0 mA	σ_0 cm	σ_t cm	σ_E/σ_{E0}
Collision mode				
86.1	9.15	1.6	6.3	3.1
79.1	9.15	2.0	6.5	3.1
70	8.1	3.2	6.7	3.0
60	6.9	3.5	7.0	3.0
50	5.8	3.7	7.4	2.9
40	4.6	3.9	7.7	2.9
30	3.5	4.1	8.1	2.8
22	2.5	4.2	8.3	2.8
Accelerating mode				
70	9.15	3.2	6.8	3.3
60	"	3.5	7.4	3.4
50	"	3.6	7.9	3.5
40	"	3.7	8.5	3.8
30	"	3.8	9.2	4.3
22	"	3.7	9.6	4.9

7 Modes of oscillation:

Coherent bunch oscillations can be described by two independent types of modes: the bunch shape modes (labelled with m) describing the distortion of the bunch itself and the coupled bunch modes (labelled with n) describing the motion of different bunches relative to each other. The longitudinal shape modes [19] consist of the dipole mode (m = 1), the quadrupole mode (m = 2) etc. In the transverse case we have the different head tail modes[1].

The spectrum of these modes consists of lines

$$\omega_p = \omega_o\ (k \cdot k_b + n + mQ_s) = \omega_o\ (p + mQ_s) \tag{7.1}$$

in the longitudinal case[19] and

$$\omega_p = \omega_o(k.k_b + n + Q) = \omega_o(p + mQ) \tag{7.2}$$

for the transverse case[1].

For the bunch shape modes we take sinosoidal modes[1] as an approximation for all cases to simplify the computation[20]. The full length L of the sinosoidal bunch is adjusted such that the peak and average current are the same as in the original bunch. This results in L = 3.93 σ for approximating a Gaussian bunch (4.2) and L = 4.89 σ for approximating the bunch (5.2) in the double RF-system.

The power spectra $h_m(\omega)$ of the different modes are shown in fig. 2. For the transverse modes (head tail modes) the effect of finite chromaticity $\xi = \frac{dQ}{Q} \Big/ \frac{dp}{p}$ has to be taken into account. This shifts the mode spectrum by $\omega_\xi = \frac{\xi Q \omega_o}{\alpha}$ and $h_m(\omega - \omega_\xi)$ must be used as indicated in fig. 2.

8 Longitudinal coupled bunch mode instabilities

These instabilities are calculated for the case of a single RF-system only, since the corresponding theory for double RF-system has not yet been developed. However the results are expected to be not very different for a double RF-system. The phase-oscillator frequency shift $\Delta\omega_{mn}$ is given by 19, 20)

$$\Delta\omega_{mn} = j\,\frac{m\,\omega_s}{m+1}\;\frac{8 I_o \pi^3}{3 k_b h V_o|\cos\phi_s|}\left(\frac{R}{L}\right)^3 \frac{\sum_k \frac{Z_L}{r}(\omega_p)\,h_m(\omega_p)}{\sum_k h_m(\omega_p)} \qquad (8.11)$$

where ω_p is given by (7.1). For the coupled bunch modes the summation goes over k in (7.1); the single bunch modes are given by

$$\Delta\omega_m = \frac{1}{k_b}\sum_{n=o}^{k_b-1}\Delta\omega_{mn}$$

For the resonator impedance and sinosoidal modes the sum (8.1) can be expressed analytically[22].

The frequency shifts (8.1) have been computed using the program EBI[20]. The results obtained for longitudinal impedances listed in table 1a) and 1c) are shown in table 4 for the dipole mode with full current at 22 and 79 GeV. The real coherent frequency shifts are much smaller than the phase-oscillation frequency itself and therefore of no concern. The growth rates are rather small because the induced currents decay considerably between the passage of successive bunches for the assumed impedance having a relatively low quality factor $Q_r \simeq 3000$.

The impedance of the fundamental mode in the RF cavities extends over several harmonics of the revolution frequency and drives coupled bunch mode instabilities. The growth rates and frequency shifts are listed in table 5 for the dipole and quadrupole mode. At the lower energies, where the higher harmonic system provides a large frequency spread, Landau damping is sufficient to stabilize all modes. However, at the higher energies this spread is smaller and Landau damping insufficient. A feed-back system will be necessary. This can be incorporated into the RF system itself, making use of the large impedance[22] to minimize the necessary power.

Table 4: Longitudinal frequency shifts and growth rates of the dipole mode for the impedances listed in table 1a) and 1c) with I_o = 9.15 mA

E GeV	$\Delta\omega_R$ s^{-1}	$-\Delta\omega_I = 1/\tau$ s^{-1}
22	584	$1.2.10^{-6}$
79	142	$3.9.10^{-7}$

Table 5: Longitudinal coupled bunch modes driven by the fundamental mode of the RF cavities with I_o = 9.15 mA

mode m	E=22 GeV		E=79GeV	
	$\Delta\omega_R$ (s^{-1})	$1/\tau$ (s^{-1})	$\Delta\omega_R$ (s^{-1})	$1/\tau$ (s^{-1})
1	-1748	716	-1234	161
2	-1774	8.4	-51	30

9) Transverse instabilities

9.1) General treatment

The betatron frequency shift due to a transverse impedance $Z_T(\omega)$ is [1)]

$$\Delta\omega_{mn} = \frac{e\,c\,I_o}{(m+1)\,2k_b\,Q\,E}\,\frac{R}{L}\,\frac{\sum Z_T(\omega_p)\,h_m(\omega_p-\omega_\xi)}{\sum h_m(\omega_p-\omega_\xi)} \qquad (9.1)$$

where ω_p is given by (7.2). For coupled bunch modes the summation goes over k in (7.2); the single bunch modes are given by

$$\Delta\omega_m = \frac{1}{k_b}\sum_{n=o}^{k_b-1}\Delta\omega_{mn}$$

9.2) Approximation for the single bunch head tail effect

For our broad band impedance the sum in (9.1) can be replaced by an integral. For the lowest mode $h_o(\omega)$ we can again use a Gaussian spectrum and get for long bunches an approximation for Q-shift of the lowest head-tail mode due to the reactive impedance Z_{TR} at $\xi \approx o$

$$\Delta Q_1 \approx \frac{e\;R^2\;I_o\;R_{TS}}{8\;k_b Q\;E\;\sigma}$$

where R_{TS} is the transverse shunt impedance of our broad band resonator impedance. Again sinosoidal modes have been assumed with a full length of 4σ.

The dependence of the growth rate of the lowest head-tail mode (m=o) on the chromaticity ξ is in this approximation

$$-\Delta \omega_{Iht} = 1/\tau_{ht} \approx \frac{c^2 e \; I_o \; R_{TS} \; \xi}{8 \; k_b \; \alpha \; E \; \omega_r}$$

where ω_r is the resonant frequency of the broad band resonator fit $\left(\frac{\omega_r}{2\pi} \sim 1.3\text{GHz}\right)$

9.3 Computations for LEP

The real frequency shift (Q-shift) and the growth rate of the single and coupled bunch mode head-tail instabilities have been calculated for LEP using the program EBI[20] with the impedances listed in table 1a) and 1c). The results obtained for $\xi = 0$ are listed in table 6. The growth rates of the coupled bunch modes are very small and can easily be stabilized by radiation damping. This is due to the large decay of the induced currents between the passage of successive bunches for the assumed resonator impedance with $Q_r \approx 3000$. The frequency shift of the lowest head tail mode (Q-shift listed in table 6) is rather large. This leads to a change of the coherent betatron frequency which is not allowed to reach an integer but is not subject to higher order resonant excitation. This Q-shift restricts the working space in the Q-diagram but is acceptable for LEP; (the coherent Q-shift in the ISR is of comparable magnitude).

The single bunch head-tail modes are strongly affected by the chromaticity ξ. The lowest mode (m=o) is damped for positive chromaticities, however higher modes could in principle be unstable under this condition. The behaviour of the latter depends on the details of the mode spectrum and the impedance function and cannot be predicted well. If the computations, listed in table 7, are taken seriously, only a range $0 \leqslant \xi \leqslant 0.0013$ for the chromaticity could be tolerated in order to get stability by radiation damping. However, higher head tail modes have never been observed in electron rings and larger positive chromaticities will probably be possible.

The instability driven by the smooth resistive wall, is small and can be neglected.

The Laslett Q shift is also small $\Delta Q_L \sim 2.10^{-3}$ with the full current at injection.

Table 6. Growth rate $\left(-\Delta \omega_I\right)$ and frequency shift (ΔQ) of the lowest head-tail mode (single and coupled) for = 0

E (GeV)	I(mA)	ΔQ	$-\Delta \omega_I = 1/\tau$ (s^{-1})
Collision mode			
86.1	9.15	-0.098	$5.5.10^{-4}$
79.1	9.15	-0.105	$5.8.10^{-4}$
70	8.1	-0.091	$5.5.10^{-4}$
60	6.9	-0.092	$4.6.10^{-4}$
50	5.8	-0.087	$4.1.10^{-4}$
40	4.6	-0.084	$3.8.10^{-4}$
30	3.5	-0.080	$3.4.10^{-4}$
22	2.5	-0.079	$3.2.10^{-4}$
Acceleration mode			
70	9.15	-0.114	$6.2.10^{-4}$
60	"	-0.115	$5.4.10^{-4}$
50	"	-0.129	$5.6.10^{-4}$
40	"	-0.152	$5.9.10^{-4}$
30	"	-0.188	$6.2.10^{-4}$
22	"	-0.246	$7.2.10^{-4}$

Table 7. Single bunch head-tail growth (or damping) rate per unit chromaticity $-d(\Delta\omega_I)/d\xi$ for I = 9.15 mA

mode m	$-d(\Delta\omega_I)/d\xi$ s^{-1}	
	E = 22GeV	E = 79GeV
0	- 34100	- 16200
1	- 20500	- 4700
2	- 95000	+ 2700
3	+ 2200	+ 2200

10. Other instabilities

There are some instabilities which could not be investigated here.

A coherent coupled bunch instability involving both beams could occur. Its strength has not been estimated but it could probably be stabilized easily with a feed back system. Having only 4 widely spaced bunches in each beam, the number of possible coupled modes is small and does not require a very wide band feed back system.

A vertical, single bunch instability has been observed in SPEAR[23)] and PETRA[18)]. This instability depends very little on the betatron tune and on the chromaticity and shows no or only a small amount of coherent signals. It is not yet understood and could not be estimated for LEP.

A so-called flip-flop effect[24)] was observed at SPEAR under conditions where two strong beams were colliding. It depends strongly on the relative phase of the two RF cavities and on the horizontal dispersion in the interaction region. The higher harmonic cavity, which is operating in SPEAR, makes this effect more difficult to control. The effect is not well understood but we hope that it is weaker for a symmetric and well distributed RF system.

11. Conclusions

Bunch lengthening is expected to be quite large in LEP but should have little influence on the performance.

The transverse coherent Q-shift can reach -0.25 at injection. The working point has to be chosen such that the coherent Q-value does not reach on integer.

The fundamental mode of the RF cavities can drive coupled bunch mode instabilities. A feed-back system will be necessary for stabilization. It can be incorporated into the RF system itself.

Coupled bunch mode instabilities driven by other impedances are weak and easily stabilized by radiation damping. In spite of this a general longitudinal and transverse feed back system should be built, since this can be done easily for a machine with only 4 bunches.

References

1) F.J. Sacherer, Proc. International Conf. on High Energy Accelerators, Stanford, 1974 (CONF 740522, USAEC, Washington, 1974), p. 347
2) H.G. Hereward, private communication
3) P.B. Wilson et al., IEEE Trans Nucl. Sci. NS-24 (1977) 1211
4) M. Bassetti et al. DESY 79/07 (1979)
5) P.B. Wilson, LEP-70/41
6) P.B. Wilson, LEP-70/69
7) E. Keil, Nuclear Instr. Meth. 100 (1972) 419
8) K. Halbach and R.F. Holsinger, Part. Accel. 7 (1976) 213
9) W. Schnell, CERN/ISR-RF/70-7 (1970)
10) Laslett
11) P.B. Wilson, PEP-233 (1977)
12) Hansen et al. IEEE Trans. Nucl. Sci. NS-22, (1975) 1381
13) A. Hofmann, F. Pedersen, Proc. 1979 Part. Accel. Conf., San Francisco (1979)
14) D. Boussard, CERN Lab. II/RF/Int./75-2 (1975)
15) E. Keil, W. Schnell, CERN Int. Rep. ISR-TH-RF/69-48 (1969)
16) M. Month, E. Messerschmid, IEEE Trans. Nucl. Sci. NS-24 (1977) 1208
17) P. Bramham et al., LEP-70/25
18) R.D. Kohaupt, Proc. 1979 Part. Accel. Conf., San Francisco (1979), Session F 7
19) F.J. Sacherer, IEEE Trans. Nucl. Sci. NS-24 (1977) 1393
20) A. Hofmann, K. Hubner, B. Zotter, Proc. 1979 Part. Accel. Conf., San Francisco (1979), Session F 20
21) B. Zotter, CERN Internal Report ISR-TH/78-16, 1978
22) J.R.J. BENNETT et al. CERN 77-14 (1977)
23) SPEAR Group; M.A. Allen et al., IEEE Trans. Nucl. Sci. NS-22 (1975) 1366
24) M. Donald and J.M. Paterson, 1979 Part. Accel. Conf., San Francisco (1979) Session M 31

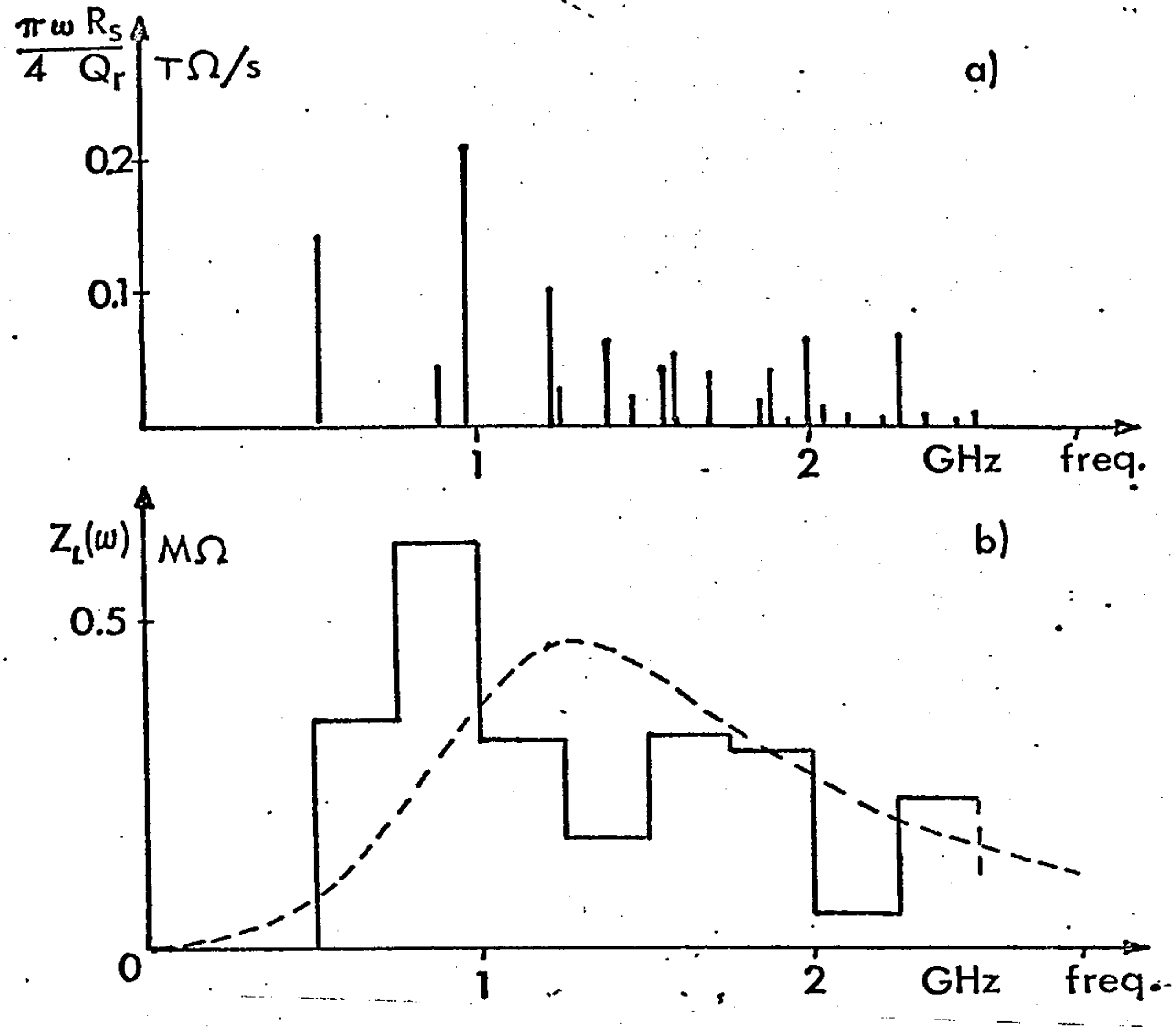

Fig. 1 a) Half areas of the computed parasitic modes

b) Averaged impedance with a fit by a Q_r = 1 resonator

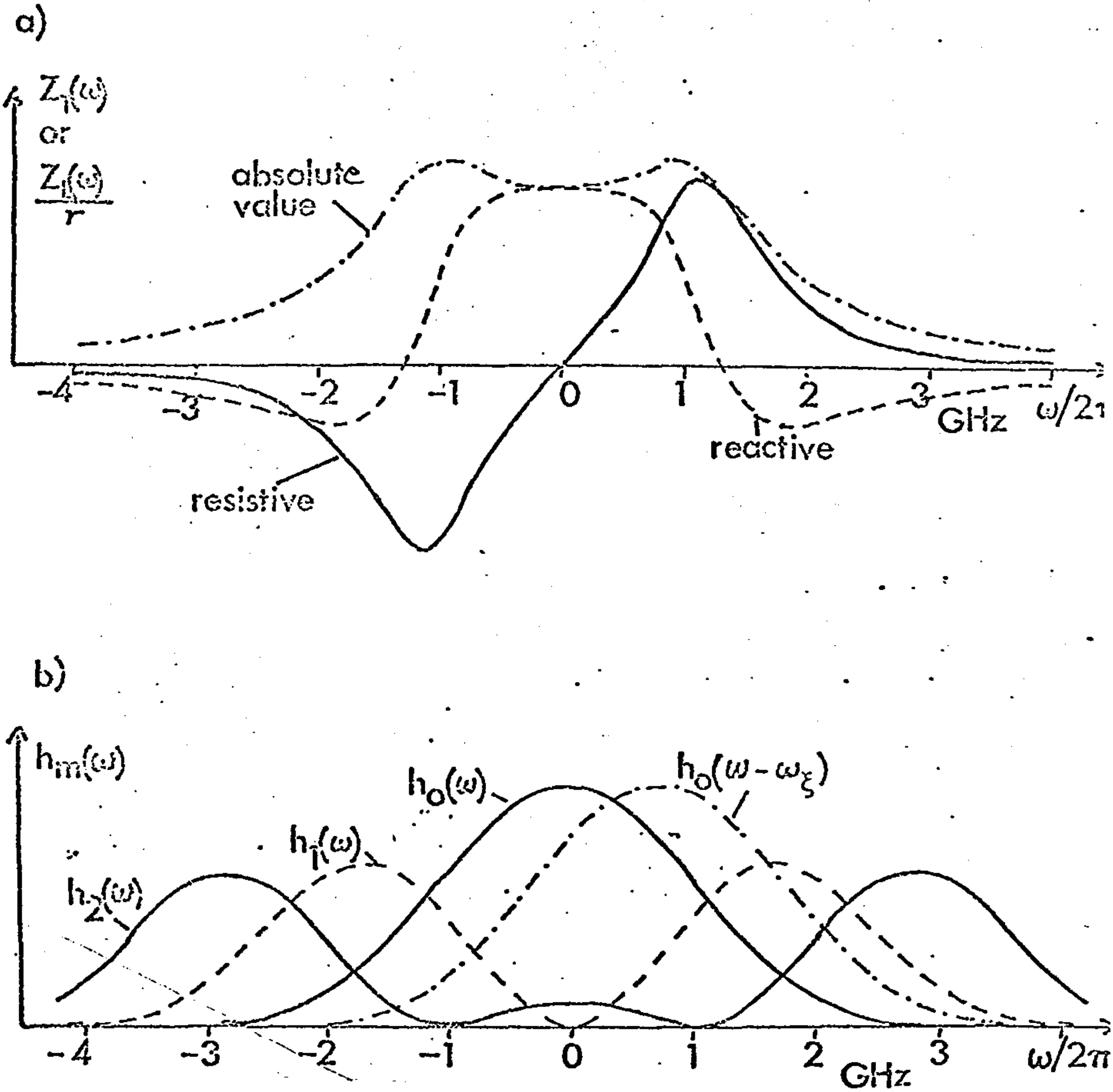

Fig. 2 a) Impedance of a resonator with $Q_r = 1$

b) Envelope of the power spectrum $h_m(\omega)$ for sinosoidal modes

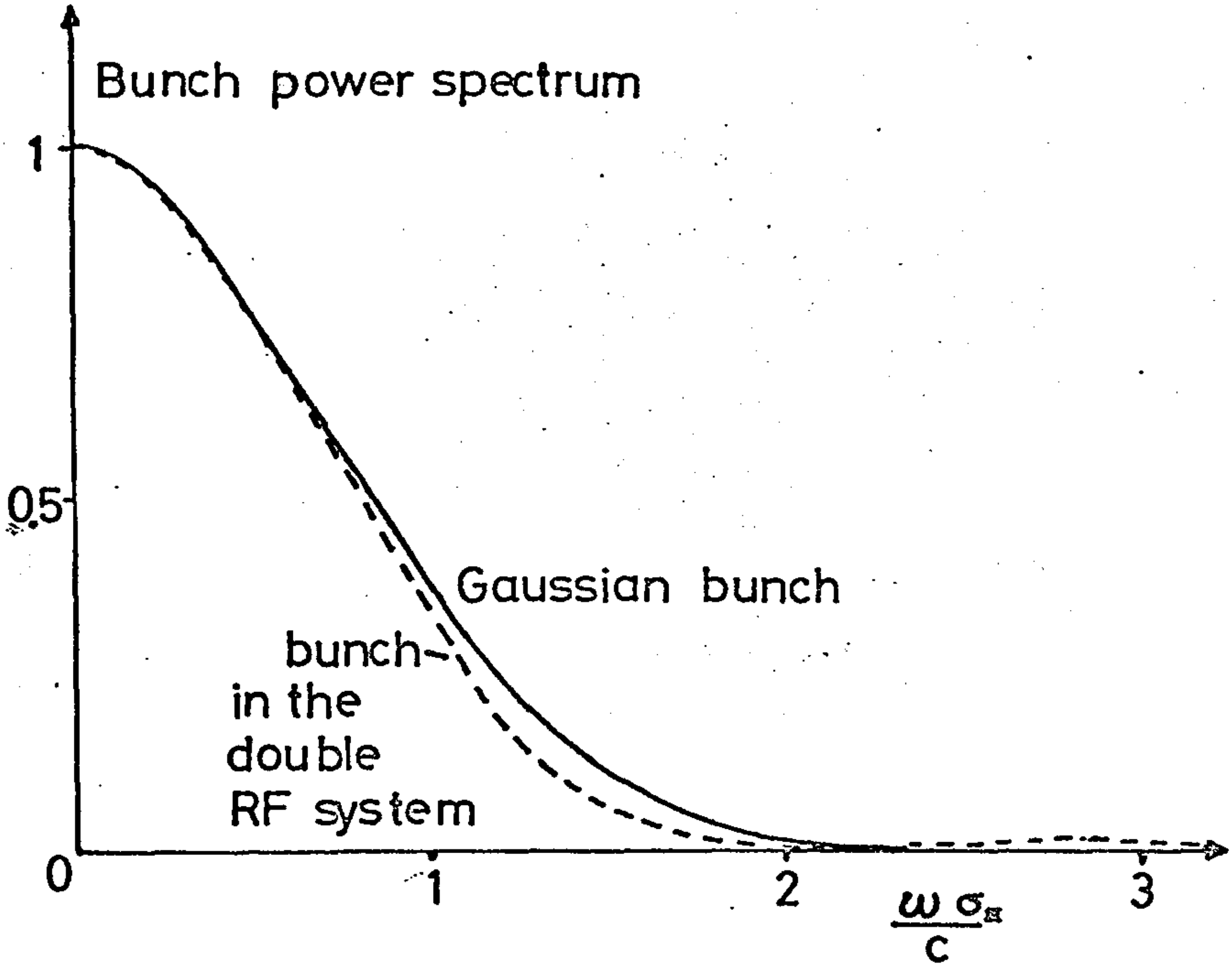

Fig. 3 Power spectrum of the approximated bunch form in the double RF system compared with the power spectrum of a Gaussian bunch